

Assessing the Effect of Saltwater Intrusion on Petroleum Hydrocarbons Plumes Via Numerical Modelling

M. Mastrocicco · N. Colombani · C. Sbarbati ·
M. Petitta

Received: 11 October 2011 / Accepted: 3 May 2012 / Published online: 17 May 2012
© Springer Science+Business Media B.V. 2012

Abstract A contamination by petroleum hydrocarbons was detected in a sandy aquifer below a petrochemical plant in Southern Italy. The site is located near the coastline and bordered by canals which, together with pumping wells, control submarine groundwater discharge toward the sea and seawater intrusion (SWI) inland. In this study, a three-dimensional flow and transport model was developed using SEAWAT-4.0 to simulate the density-dependent groundwater flow system. Equivalent freshwater heads from 246 piezometers were employed to calibrate the flow simulation, while salinity in 193 piezometers was used to calibrate the conservative transport. A second dissolved species, total petroleum hydrocarbons (TPH), was included in the numerical model to simulate the plumes originating from light non-aqueous-phase liquid. A detailed field investigation was performed in order to determine the fate of dissolved hydrocarbons. Fifteen depth profiles obtained from multilevel samplers (MLS) were used to improve the conceptual model, originally built using a standard monitoring technique with integrated depth sampling (IDS) of

salinity and TPH concentrations. The calibrated simulation emphasises that density-dependent flow has a great influence on the migration pattern of the hydrocarbons plume. This study confirms that calibration of density-dependent models in sites affected by SWI can be successfully reached only with MLS data, while standard IDS data can lead to misleading results. Thus, it is recommended to include MLS in the characterization protocols of contaminated sites affected by SWI, in order to properly manage environmental pollution problems of coastal zones.

Keywords Modelling · Variable density · Seawater intrusion · Hydrocarbons · Multilevel sampling

1 Introduction

The most densely populated regions, all over the world, are located along the coastlines, since they normally provide the best conditions both for economic development and quality of life. The integrity of coastal waters is threatened not only by activities occurring directly in the waters but even by industrial, agricultural and land use practices located throughout watersheds contributing to the coastal waters. One of the consequences is that polluted groundwater may have a significant influence on coastal ecosystems, especially at high concentration or where submarine groundwater discharge (SGWD) is an important term of hydrogeological budget. Several studies have indicated that SGWD can be a significant

M. Mastrocicco · N. Colombani (✉)
Department of Earth Sciences, University of Ferrara,
Ferrara, Italy
e-mail: clo@unife.it

C. Sbarbati · M. Petitta
Department of Earth Sciences,
University “Sapienza” of Rome,
Rome, Italy

component of the total discharge to the coasts (Cambareri and Eichner 1998; Moore 1999; Reilly and Goodman 1985). Field studies have shown that a variety of contaminants can reach the shoreline through SGWD (Buddemeier 1996; Simmons 1992; Robinson et al. 1998), i.e. nutrients and pesticides from intensive agricultural practice (Gallagher et al. 1996; Ullman et al. 2003; Valiela et al. 1992), organic matters from septic tanks (Weiskel and Howes 1992), trace metals and petroleum hydrocarbons from industrial activities (Ataie-Ashtiani et al. 2002; Dausman et al. 2010; Mao et al. 2006).

Nevertheless, the effects of contaminated groundwater on coastal environments are not as well-known as those of river and storm water. Thus, in these areas, groundwater management and protection are gaining increasing attention not only for the high probability to observe a contamination along the coast but also for the high intrinsic ecological value of coastal systems, for the fresh water barrier effect against aquifer salinization and for the large storage capacity of coastal aquifers which could be exploited as a source of water supply (Barlow and Reichard 2010). In fact, long-term planning of land use and groundwater management are required to ensure a sustainable groundwater resource use to be maintained for future utilization, whilst enabling an acceptable demographic, commercial and industrial development (Bear et al. 1999; Praveena and Aris 2010).

Groundwater flow and contaminant transport in coastal aquifers are fairly complicated. The major factors affecting coastal groundwater flow systems include: tides, moving boundary conditions, beach slope and beach seepage dynamics, density variable flow and the relationship between saltwater–freshwater interface induced by sea water intrusion (SWI, Ataie-Ashtiani et al. 1999; Baird and Horn 1996; Li et al. 1999; Naji et al. 1998). Interactions between freshwater and seawater through coastal aquifers may be driven by a seaward hydraulic gradient, i.e. fresh SGWD near the shoreline, and by a variable density flow causing the mixing of fresh groundwater and seawater.

The study of density contrast effect on groundwater flow and contaminant transport in coastal aquifers is a crucial part of the investigation on pollution pathways along coastlines to coastal water bodies. It was shown that density contrast has a significant effect on the spatial distribution of contamination in the aquifer near the shoreline (Simmons et al. 2001). An improved understanding of the influence of density contrast between

saltwater and freshwater on contaminant movement could allow better strategies to be implemented to control or mitigate the effects on coastal wetlands, coastal aquifers and the adjacent marine environment.

Numerical models that account for the effects of fluid density on groundwater flow are being used more and more frequently to address scientific, engineering and water resource management problems (Giambastiani et al. 2007; Oude Essink 2001; Xue et al. 1995) in coastal aquifer where a unique combination of factors leads to complicated hydrodynamic conditions (Kolditz et al. 1998; Naji et al. 1998; Oude Essink 2001). A major contribution to the study of contaminant transport in coastal aquifers came from Zhang et al. (2001, 2002) and Volker et al. (2002). By experimental and mathematical modelling, including in the simulations the seawater density, they found that the contaminant plume's shape is affected only near the mixing zone of saltwater and freshwater. While away from this zone, contaminant plume migration is barely influenced by saltwater–freshwater interaction and seawater density and tidal variations could be neglected. Moreover, the occurrence of a density contrast on the groundwater circulation does not change the total amount of land-derived chemical input to the sea over a long period, but may change the flowpath of groundwater and the discharge point of contaminant fluxes (Volker et al. 2002). However, three-dimensional modelling is usually computationally time consuming when multi-species variable density flow and transport are simulated.

In addition, the field data required for the implementation and calibration of three-dimensional variable density models are usually more complex to be obtained than the ones needed for simple flow models (Abarca et al. 2007; Shoemaker 2004) because of the need to characterize the aquifer not only in terms of hydrodynamic parameters but also from a hydrochemical point of view. Thus, a key issue to understand salinization processes and contaminants migration in density-driven systems is to correctly characterize the vertical variability of groundwater quality (Henderson et al. 2009; Netzer et al. 2011). Despite this, the sampling protocols followed in many contaminated sites do not still make use of multilevel sampling (MLS) techniques for economic reasons (Dietze and Dietrich 2011; Einarson and Cherry 2002) even if the integrated depth sampling (IDS) protocols could mask the vertical distribution of contaminants.

Many of the abovementioned studies face the problem of SGWD from a theoretical point of view or thanks to well-designed laboratory experiments (Luyun et al. 2009), but less work has been done on contaminant transport in real field sites affected by SWI. The objectives of this work are (1) to investigate the influence of the density-dependent flow on the migration pattern of total petroleum hydrocarbons (TPH) plumes in an intensively characterized site and (2) to assess the benefit or worsening in adding the IDS concentrations of salinity and TPH obtained by MLS profiles in the calibration procedure of the numerical model.

2 Materials and Methods

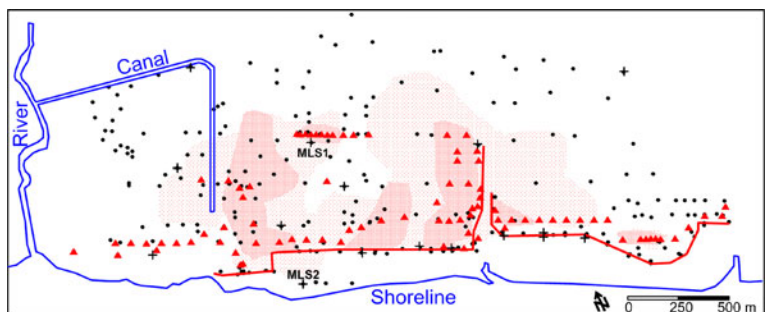
2.1 Site Description

The study site is a petrochemical plant in Italy located near the shoreline (Fig. 1). An unconfined aquifer consisting of sandy and sandy-loam deposits is present below the site; this aquifer has a variable thickness from 10 m inland to 30 m near the shore line and becomes semi-confined by silty-clay sediments inland (Fig. 2). Below this aquifer there is an aquitard level consisting of over consolidated silty-clay sediments with thickness from 7 to 25 m. This unit contains a local and confined sandy aquifer layer (5 m thick) situated in the western part of the site. The hydrostratigraphic sequence ends up with an aquiclude consisting of clays (basal clay in Fig. 2). The local confined aquifer is completely separated from the unconfined and polluted aquifer, as confirmed by several multi-aquifer pumping tests and from differences in hydraulic heads of more than 1 m between the confined and unconfined aquifer. The hydrostratigraphic sketch in Fig. 2 shows a simplified view, based on the groundwater circulation at the scale of the site, of the geometry of the system, reconstructed by the

interpolation of more than 870 core logs. The hydraulic parameters, saturated hydraulic conductivity (K), specific storage (S_s) and specific yield (S_y) of each hydrostratigraphic unit was estimated via pumping tests and slug tests at different locations. Over 70 pumping test data indicate that K is log normal distributed in the contaminated unconfined aquifer, with an geometric mean value of 18 m/day.

Hydraulic head contouring (Fig. 3) indicates a groundwater flow system naturally discharging towards the shoreline, but affected by the interaction with river and canal levels and by the influence of the horizontal flow barrier (HFB) and of the pumping wells of the hydraulic barrier (HB), active since 2002 to prevent the migration of contaminants outside of the site boundaries. The HB consists in an alignment of 67 fully screened pumping wells along the shore line (Fig. 1); the barrier are hosts in the unconfined aquifer, and the extraction rate ranges from about 60 l/s. The HFB consists of a vertical bentonite wall (1 m thick) enclosed by plastic sheet piles emplaced by a trenching crane, with a permeability of $1e-5$ m/day. The HFB is keyed in the aquitard in the eastern part of the site, while in the western part the HFB is not keyed because the aquitard is too deep. The canal, placed perpendicularly to the shore line (Fig. 1), supplies seawater necessary for cooling plant purpose. The canal is well connected with the unconfined aquifer as shown in a previous study (Mastrocicco et al. 2011) and thus creates a seawater plume in the aquifer. On the other hand, the river, which lays on the western side of the site (Fig. 1), has little interaction with the unconfined aquifer. Direct recharge, approximately 70 mm/year, was estimated to occur over most of the study area. The presence of TPH in the unconfined aquifer underlying the plant was

Fig. 1 Schematic representation of the site: location of monitoring piezometers (black circles), MLS (black crosses), pumping wells (red triangles), HFB (red lines), LNAPL pools (red shaded areas in August 2010, red dotted areas in August 2002). MLS1 and MLS2 refer to Fig. 8



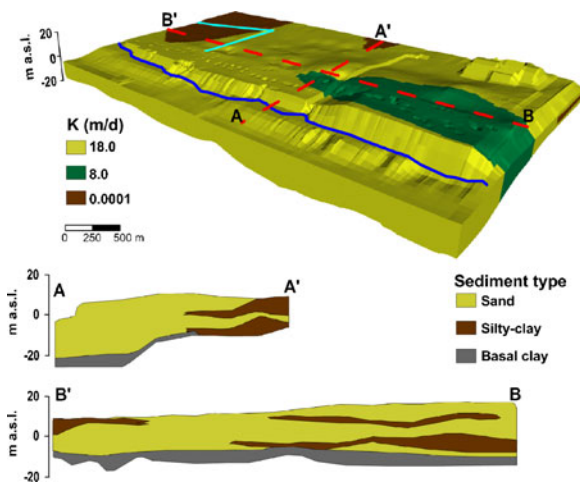
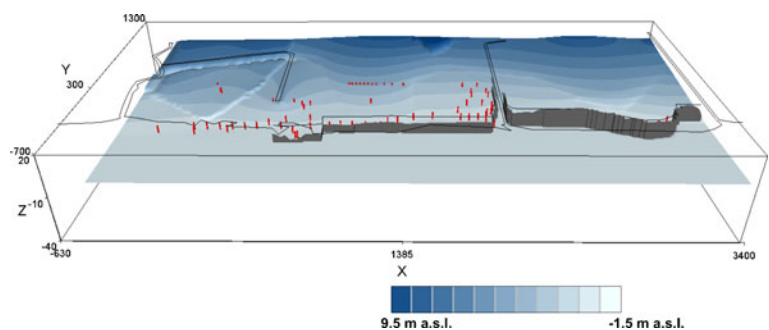


Fig. 2 Three-dimensional hydrostratigraphic sketch of the site with different horizontal hydraulic conductivity zones assigned to the numerical model (*upper panel*) and two perpendicular geological sections (*lower panel*). The coast line is represented by the *blue line*, and the seawater canal is shown by the *light blue line*. Vertical exaggeration is 1:10

due to past leakage from tanks and pipes located in the unsaturated zone. An unknown volume of light non-aqueous-phase liquid (LNAPL)-containing TPH was released in the past decades, and over time, LNAPL supernatant phase migrated following the piezometric gradient. The LNAPL-contaminated zone is systematically shrinking in time as a result of remediation strategies. At the beginning of 2002, the estimated areal extension of the LNAPL was 1.2 km², while in 2010 reduced to 0.52 km² (Fig. 1).

The supernatant LNAPL source is a mixture of petroleum hydrocarbons, highly variable from place to place. More than 70 LNAPL samples were analysed and 32 resulted crude oil, 17 presented aromatics hydrocarbons (mainly BTEX) while 23 were a mixture between the previous

Fig. 3 Three-dimensional contour plot of calculated heads, HFB is evidenced by *grey wall* and pumping wells by *red cylinders*. Vertical exaggeration is 1:20



two. In August 2010, 15 piezometers throughout the site (Fig. 1) were selected and sampled to define concentration profiles within the contaminated unconfined aquifer.

2.2 Sampling and Analytical Methods

Since 2003, 246 monitoring piezometers located within the study domain, screened between 10 and 25 m below ground level, have been monitored every month for piezometric level, LNAPL apparent thickness, physical–chemical parameters and pollutant concentration.

Groundwater was sampled from standard fully screened piezometers equipped with straddle inflatable packers Solinst for depth profiles. The packer assembly consisted of a 30-cm-long sampling port, set in the middle of two inflatable packers, a peristaltic pump used for low-flow purging and an inertial Waterra pump for gas and volatile compounds sampling dissolved in groundwater. From each piezometer (4-in. diameter) three to five samples have been collected at different depths, depending on the screen length. MLSs were purged for three volumes (approximately 5 l) at low flow rates (≈ 1 l/min) until pH, dissolved oxygen (DO) and E_h stabilized and filtered through a 0.45- μ m filter, prior to collection of a groundwater sample in glass vials with no head space. Field parameters were determined towards the end of purging using a multi-parameter probe WTW Multi 340i which included a SentiTix 41 pH combined electrode with a built-in temperature sensor for pH measurement, a CelloX 325 galvanic oxygen sensor for DO measurement, a combined AgCl–Pt electrode for E_h measurement and a Tetracon 325 4-electrode conductivity cell for EC measurements. Chloride (Cl⁻) was determined by ion chromatography with ICS-2000 Dionex, and TPH was analysed via gas chromatography–mass spectrometry ThermoElectron MAT95 XP.

3 Numerical Flow and Solute Transport Models

3.1 Three-Dimensional Flow Model Setup

Integrating all the existing site-specific hydrogeological information, a three-dimensional, steady-state groundwater flow model was developed to understand the general flow pattern at the site. The USGS flow model SEAWAT-4.0 (Langevin et al. 2007) was used. SEAWAT-4.0 is a coupled version of MODFLOW and MT3DMS designed to simulate three-dimensional, variable density, saturated groundwater flow and transport of dissolved species. Conversion between head as measured by the native aquifer water and equivalent freshwater head is necessary in converting model results. SEAWAT-4.0 automatically converts input data to equivalent freshwater head and automatically converts equivalent freshwater head to actual head before writing to output files. The model domain extends over an area of 5.1 km², and it is discretized according an irregular spaced grid from 20×20 to 2×2 m close to the pumping wells, with a gradual decrease of cell size using a 1.5 ratio to avoid numerical oscillation. Vertically the model domain is discretized into 12 layers of different thicknesses, from 12.5 m above sea level (a.s.l.) to -30 m a.s.l. The top of the grid is represented by the local ground surface, ranging from -3 to 12.5 m a.s.l.; the bottom of the grid, representing the top of the underlying aquiclude (the basal clay unit), ranges from -20 to -30 m a.s.l., as deduced from stratigraphic logs (Fig. 2). Table 1 lists the pre-calibration hydraulic parameters values used in the model.

The initial pre-calibration estimates of the K distribution have been determined from geologic logs, pumping tests, and slug tests in 70 wells and heat pulse flow meter measurements in five piezometers. Anisotropy ratio between horizontal and vertical K is set to 5, since no evidence was found to support strong vertical or horizontal anisotropy.

The Constant Head Boundary package was used to represent the northern regional flow boundary and the southern shoreline; the recorded pumping rates were incorporated for each well of the HB using the Well package; the River package was employed to simulate the river and an internal canal connected with groundwater; by mean of the Recharge package, a recharge rate of 70 mm/year was assigned to all the domain, according to the historical data (from 2000 to 2010) of

Table 1 Hydraulic parameters used in the three-dimensional flow and transport model

Parameter	Values
Unconfined aquifer sand K (m/day)	18
Unconfined aquifer sand S_s (1/m)	1e ⁻⁴
Unconfined aquifer sand S_y (-)	0.3
Unconfined aquifer silty sand K (m/day)	8
Unconfined aquifer silty sand S_s (1/m)	1e ⁻⁵
Unconfined aquifer silty sand S_y (-)	0.2
Unconfined aquifer silty-clay K (m/day)	1e ⁻⁴
Unconfined aquifer silty-clay S_s (1/m)	1e ⁻⁶
Unconfined aquifer silty clay S_y (-)	0.1
River conductance C (m ² /day)	200

598 mm/year of mean precipitation and 17.9°C of mean temperature recorded within the site.

The automated inverse model PEST (Doherty 2002) was used to obtain best estimates for the recharge rate, the K values and the conductances of river and canal determining the rate of water exchange between surface bodies and the unconfined polluted aquifer. Prior information on isotropic distribution of K_x and K_y values and on the ratio between horizontal and vertical K values was used in order to constrain parameters estimation; the objective function consisted of all available piezometric heads, recorded in August 2010 from 246 observation piezometers. Each screen interval was subdivided with the layer proportion to ensure that calculated heads were related to the observed heads. If an observation borehole is screened over more than one model layer, and the observed hydraulic head is affected by all screened layers, then the associated simulated value is a weighted average of the calculated hydraulic heads of the screened layers.

3.2 Three-Dimensional Transport Model Setup

A non-reactive transport model was used to investigate the effect of SWI on contaminant fate and in particular to determine the possible mass flux of contaminant discharge to the coastline. SEAWAT-4.0 was used to simulate the interaction between SWI and the TPH plumes, taking into account the effect of variable density transport processes.

For the contaminant transport, no chemical reactions were considered since this study is planned to investigate physical control on conservative chemical

transport. This assumption holds since the biodegradation potential at this location is very low, as indicated by MLS hydrogeochemical data (Mastroicco et al. 2011). Dissolved Cl^- was selected as environmental tracer to track SWI, while TPH was selected to track the overall bulk dissolved plumes. Both Cl^- and TPH were used for model calibration.

The concentration distribution of the TPH phase zones was simulated by means of Constant Concentration package after the verification of equilibrium dissolution between the aqueous phases and LNAPL. Verification consisted in analysing the composition of the LNAPL source and of the dissolved species in groundwater samples collected beneath the LNAPL, in three piezometers with different LNAPL composition. The LNAPL species were then converted into theoretical aqueous concentration using the Raoult law for multi-component solubility. Since the theoretical concentrations were very well correlated (coefficient of determination $R^2=0.97$ and its calculated probability $p<0.05$) with observed aqueous concentrations, the assumption of constant release from the LNAPL source can be applied at this site. Recharge water composition was assumed to have null TPH concentration and 200 mg/l of Cl^- after percolation through the unsaturated zone as observed in most of piezometers located near the northern boundary. The Constant Concentration package (in which density was correlated by a linear function with Cl^-) was used to simulate the sea boundary with a Cl^- concentration of 19 g/l; the northeastern corner of the site where a marsh swamp is present has a Cl^- concentration of 11 g/l.

Time was subdivided into two stress periods: the first of 7,300 time steps of equal length (1 day each for 20 years), to accurately simulate SWI and TPH plumes development; the second stress period was subdivided in 2,920 time steps of equal length (1 day each for 8 years), to simulate the effect of partially penetrating pumping wells, representing the HB. Simulation time ensured that steady-state conditions were reached with respect to heads and concentrations. Tidal fluctuations were not included in the simulation holding that in this area of the Mediterranean sea, tides magnitude is known to be minimal and could be neglected (Sammarì et al. 2006). Each screen interval was subdivided with the layer proportion to ensure that calculated concentrations were related to the observed concentrations. If an observation borehole is screened over more than one model layer (IDS), and the observed

concentration is affected by all screened layers, then the associated simulated value is a weighted average of the calculated concentration of the screened layers. The grid discretization was tested for numerical dispersion by reducing the thickness of layers by a factor 2. No appreciable variation of the results occurred between the two different discretization levels. Different numerical resolution methods were tested, and the hybrid method of characteristics (Zheng and Bennett 2002) was found to be the most accurate to avoid numerical dispersion.

4 Results and Discussion

4.1 Site-Wide Three-Dimensional Density-Dependent Flow and Transport Model

From Fig. 3, it is evident that the groundwater flow is mainly perpendicular to the shoreline even if local perturbation of the dominant flow direction are detectable in proximity of the pumping wells and of the HFB. In addition, the canal's reach perpendicular to the shoreline is hydraulically connected to the unconfined aquifer while the canal's reach sub-parallel to the shoreline, bounded by silty-clay materials (Fig. 2), does not exchange water with the unconfined aquifer.

The calibrated canal and river conductances are very large (200 m^2/day), suggesting a high connection between surface water bodies and groundwater, while the optimized recharge rate results 82 mm/year and the optimized K value for the unconfined aquifer is 18 m/day. The latter value is very similar to the geometric mean obtained by aquifer testing. The calibration statistics (R^2 of 0.94 and absolute mean error of 0.41 m) and the relationship between computed and observed heads are to be considered good (Fig. 4).

Since the canal is continuously supplied of seawater for plant cooling purposes, the canal leakage produces a plume of seawater in the aquifer, accordingly to the MLS profiles which allowed identifying this pattern with respect to the IDS data set that failed in registering it. In fact, the modelled seawater plume migrates downward toward the aquifer bottom, driven by the density contrast between fresh groundwater and seawater; then, it migrates downgradient following the forced head gradient imposed by the HB and the slope of the unconfined aquifer bottom which bends toward the sea.

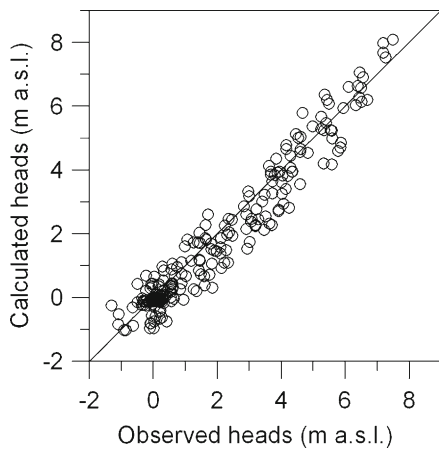


Fig. 4 Scatter diagram of the observed versus calculated heads

Figure 5 also shows that the saltwater wedge develops inland for a short distance (approximately 200 m from the shoreline) for two different reasons: the presence of the HFB which prevents a further migration inland and the SGWD contrasting the SWI where the HFB is not present. For these reasons, SWI never reaches the background brackish water originating from the marsh swamp in the northeastern portion of the domain.

Accordingly, close to the canal, the modelled dissolved TPH plume dives downgradient carried down

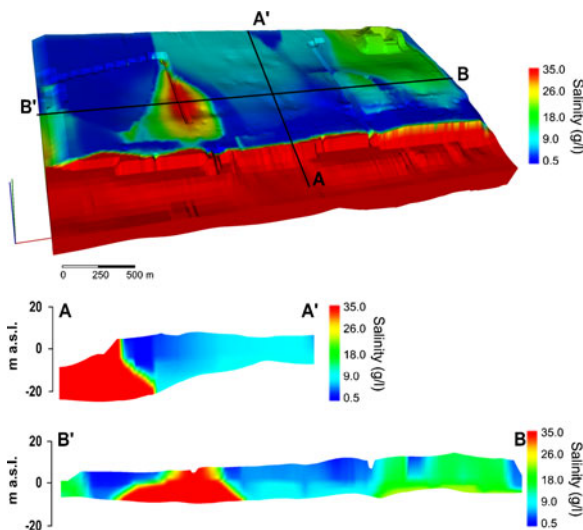


Fig. 5 Three-dimensional solid contour maps of calculated concentrations for salinity (*upper panel*) and two sections perpendicular and parallel to the shoreline (*lower panel*). Location of the sections is shown in the *upper panel*. Vertical exaggeration is 1:10

by the seawater coming from the leaking canal (Fig. 6), but cannot discharge to the shoreline because of the effect of the HFB, which prevents the migration toward the sea boundary. The presence of the SWI and of the seawater leaking from the canal does not significantly affect net mass discharge towards the shoreline from the perspective of solutes mass balance in the long term, but cause a differently distributed SGWD over the aquifer depth.

A major consequence that results from the occurrence of seawater leaking from the canal is that the TPH plume does not travel upwards towards the shore along the freshwater–saltwater interface (vertical flow) exiting in the shallow part of the aquifer, as expected if only SWI was present at the site (Volker et al. 2002). Instead, the TPH plume is forced to flow in the bottom part of the aquifer as a result of the density contrast effect due to the seawater leaking from the canal.

In the first case, the sole use of the HB should have been selected as remediation strategy, since the TPH plume travelling in the shallow portion of the aquifer would have been completely intercepted by the pumping wells and prevented to migrate toward the shoreline. In the latter case, the TPH plume which dives down forced by the seawater leaking from the canal has to be limited by the HFB in order to prevent its migration

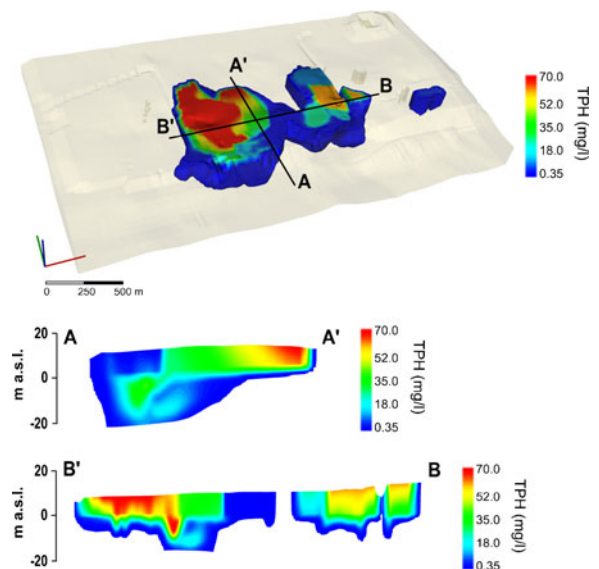


Fig. 6 Three-dimensional solid contour maps of calculated TPH concentrations in the whole site (*upper panel*) and two sections perpendicular and parallel to the shoreline (*lower panel*). Location of the sections is shown in the *upper panel*. Vertical exaggeration is 1:10

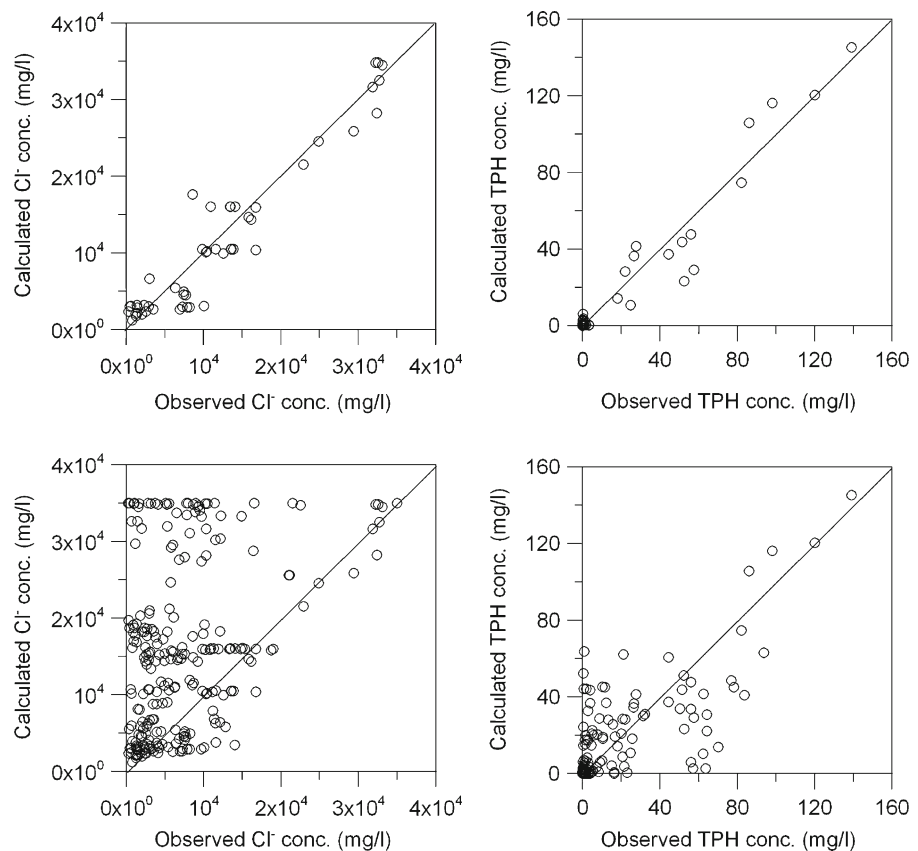
toward the shoreline. It follows that to properly identify the best remediation strategy (or protection measures) for a given site, not only density contrast effect due to natural SWI has to be accounted for to delineate the conceptual and numerical models but also artificially induced density contrast effect, i.e. the percolation of dense seawater from canal, made for plant cooling, crossing the field site. It is here essential to underline that only the MLS technique was able to witness the abovementioned behaviour of the canal, while the IDS technique failed in reconstructing a reliable conceptual model.

From the mass balance at the end of the simulation (discrepancy between in and out <1 %), the model calculates a dissolved TPH release from LNAPL of 24.6 kg/day, a mass aquifer storage (total mass of contaminant dissolved in groundwater and stored in the whole aquifer each day) of 1.6 kg/day and a recovery rate of 23.0 kg/day from the pumping wells, with a null TPH discharge towards the coastline. This confirms that the selected protection measures are actually able

to avoid the migration of TPH toward the sea, although this model does not give information on the time required to achieve the remediation goals, time which depend on the ability to remove the residual NAPL phase.

In the simulation, a satisfactory fit among the measured and calculated concentrations is found for the MLS monitoring piezometers (Fig. 7) with an R^2 of 0.91 for Cl^- and 0.93 for TPH. The Cl^- concentration profiles were used to estimate the longitudinal dispersivity (α_L), the horizontal transverse dispersivity (α_{Th}) and the vertical transverse dispersivity (α_{Tv}) that were found to be equal to 2 m, 1×10^{-3} m and 4×10^{-4} m, respectively. Holding these values, the transport model result also calibrated against the MLS TPH profiles, confirming that TPH is mainly transported conservatively at this site. From this model analysis, it cannot be excluded that biodegradation occurs in limited portions of the site or for highly degradable compounds (like toluene), but the results of TPH analyses suggest conservative transport since a good model fit was achieved not including degradation.

Fig. 7 Scatter plots of calculated and observed concentration for Cl^- and TPH with MLS (*upper panels*) and with IDS added to MLS (*lower panels*)



The attempt to include the IDS dataset in the calibration procedure (Fig. 7) led to a worsening in the calibration statistics, with an R^2 of 0.36 for Cl^- and 0.55 for TPH. In particular, Fig. 8 shows observed data and the calculated values on two representative MLS located along a possible flow line (see Fig. 1 for their location). In the MLS1, located downgradient to fully screened pumping wells, a clear vertical zonation of both TPH and Cl^- concentration profiles is not appreciable, because the long screen wells mix groundwater along the entire aquifer section and homogenized the concentrations within the aquifer profile. On the contrary, the MLS2 shows a different situation, with increased Cl^- concentrations from the top to the aquifer's bottom due to saltwater intrusion and TPH profile showing a double peak. While the MLS1 data do not differ substantially from IDS data, because of the well mixing effect, the MLS2 data cannot be correctly interpreted and modelled just with IDS data. This confirms that the IDS (sampling at the middle of filtered tracts) technique is not suitable to properly characterize the fate and transport of contaminants especially if a complex hydrodynamic setting is present due to the density contrast effect originated by SWI.

4.2 Sensitivity Analysis

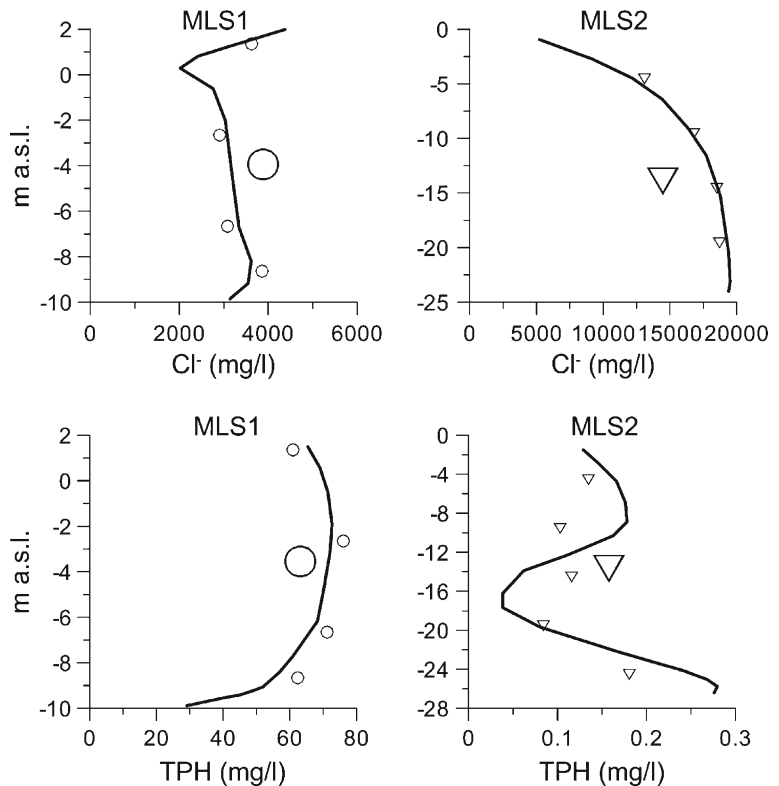
To quantify the TPH transport model sensitivity to each parameter, the normalized sensitivity coefficient (Zheng and Bennett 2002) was calculated from:

$$\Sigma_{i,k} = \frac{\Delta v_{\text{TPH}}/v_{\text{TPH}}}{\Delta p_k/p_k}$$

where p_k is the k th parameter value, Δp_k is the perturbation of the parameter value, v_{TPH} is the simulated vertically integrated TPH mass flux and Δv_{TPH} is the change of the TPH mass flux that resulted from the perturbation of parameter p_k .

The composite sensitivity was computed for a 50 % perturbation of the recharge rate, the horizontal K and the α_L . The most sensitive parameter was the recharge rate with a value of 1.9, while the least sensitive was the horizontal K with a value of 0.04, α_L showing an intermediate value of 0.32. This is due to the high impact of recharge on the calculated heads and on concentration, since it was assumed that recharge water had null TPH concentration after percolation through the unsaturated zone. Augmenting the recharge flux of 50 % led to an average head rise up to

Fig. 8 Concentration depth profiles at MLS1 and MLS2 (see Fig. 1 for location) of observed (symbols) and modelled (black lines) Cl^- (upper plots) and TPH data (lower plots). For comparison also IDS concentrations are reported with larger symbols



0.31 m and decreased the mass of TPH in the aquifer to 5.3 %.

5 Conclusions

This study addresses the influence of the density contrast between fresh groundwater and seawater on the migration pattern of total petroleum hydrocarbons plumes within an unconfined coastal aquifer, where salt water intrusion dynamics is affected by the pumping wells of the remediation facilities and by a leaking canal. This study points out that the presence of the SWI can modify the fate and transport of contaminants flowing towards the shoreline. Ignoring the density contrast between freshwater and saltwater can cause an erroneous definition of the site conceptual model. Even if the density contrast could not affect significantly the net mass discharge of TPH, it could determine a different distribution of contaminants over the aquifer depth. The employment of the MLS technique provided a dramatic improvement in the understanding of saltwater and contaminants distribution within the aquifer and allowed to implement a numerical simulation in order to verify the fate of dissolved TPH in the aquifer.

For the relatively simple stratigraphy and LNAPL distribution present at the simulated field site, the numerical model was able to successfully reproduce the observed heads and concentration distribution. A good fit with an R^2 of 0.91 for Cl^- and 0.93 for TPH was achieved using MLS for calibration, while including the IDS dataset leads to a worsening in R^2 . This study confirms that calibration of density-dependent flow and transport models in sites affected by SWI can be successfully reached only with MLS data, while standard IDS data can lead to misleading results. Thus, it is recommended to include MLS in the characterization protocols of contaminated sites affected by SWI, in order to provide accurate data on which an appropriate environmental management of the coastal zone could be established.

Acknowledgments Alessandro Lacchini and Valentina Marinelli (Department of Earth Sciences, University “Sapienza” of Rome, Italy) are acknowledged for the data base design and management.

References

- Abarca, E., Carrera, J., Sánchez-Vila, X., & Voss, C. I. (2007). Quasi-horizontal circulation cells in 3D seawater intrusion. *Journal of Hydrology*, 339, 118–129.
- Ataie-Ashtiani, B., Volker, R. E., & Lockington, D. A. (1999). Numerical and experimental study of seepage in unconfined aquifers with a periodic boundary condition. *Journal of Hydrology*, 222, 165–184.
- Ataie-Ashtiani, B., Volker, R. E., Lockington, D. A., (2002). Contaminant transport in the aquifers influenced by tide. *Australian Civil Engineering Transactions, Institution of Engineering*, Australia, CE43, 1–11.
- Baird, A. J., & Horn, D. P. (1996). Monitoring and modeling groundwater behavior in sandy beaches. *Journal of Coastal Research*, 12(3), 630–640.
- Barlow, P. M., & Reichard, E. G. (2010). Saltwater intrusion in coastal regions of North America. *Hydrogeology Journal*, 18, 247–260.
- Bear, J., Cheng, A. H.-D., Sorek, S., Ouazar, D., & Herrera, I. (1999). *Seawater intrusion in coastal aquifers—Concepts, methods and practices*. Dordrecht: Kluwer Academic Publishers.
- Buddemeier, R.W. (1996). Groundwater flux to the ocean: Definitions, data, applications, uncertainties. In: Buddemeier, R.W. (Ed.). *Groundwater discharge in the coastal zone: Proceedings of an International Symposium*. LOICZ IGBP, LOICZ/R&S/96-8, The Netherlands: Texel.
- Cambareri, T. C., & Eichner, E. M. (1998). Watershed delineation and ground water discharge to a coastal embayment. *Ground Water*, 36(4), 626–634.
- Dausman, A. M., Doherty, J., Langevin, C. D., & Dixon, J. (2010). Hypothesis testing of buoyant plume migration using a highly parameterized variable-density groundwater model at a site in Florida, USA. *Hydrogeology Journal*, 18, 147–160.
- Dietze, M., & Dietrich, P. (2011). A field comparison of BTEX mass flow rates based on integral pumping tests and point scale measurements. *Journal of Contaminant Hydrology*, 122, 1–15.
- Doherty, J. (2002). *PEST—Model-independent parameter estimation: User's manual* (5th ed.). Brisbane: Watermark Numerical Computing.
- Einarson, M. D., & Cherry, J. A. (2002). A new multilevel ground water monitoring system using multichannel tubing. *Ground Water Monitoring and Remediation*, 22, 52–65.
- Gallagher, D. L., Dietrich, A. M., Reay, W. G., Hayes, M. C., & Simmons, G. M., Jr. (1996). Ground water discharge of agricultural pesticides and nutrients to estuarine surface water. *Ground Water Monitoring and Remediation*, 16, 118–129.
- Giambastiani, B. M. S., Antonellini, M., Oude Essink, G. H. P., & Stuurman, R. J. (2007). Saltwater intrusion in the unconfined coastal aquifer of Ravenna (Italy): A numerical model. *Journal of Hydrology*, 340, 91–104.
- Henderson, T. H., Mayer, K. U., Parker, B. L., & Al, T. A. (2009). Three-dimensional density-dependent flow and multicomponent reactive transport modeling of chlorinated solvent oxidation by potassium permanganate. *Journal of Contaminant Hydrology*, 106, 195.211.

- Kolditz, O. R., Ratke, H., Diersch, G., & Zielke, W. (1998). Coupled groundwater flow and transport: 1. Verification of variable density flow and transport models. *Advances in Water Resources*, 21(1), 27–46.
- Langevin, C. D., Thorne, D. T. Jr., Dausman, A. M., Sukop, M. C., Guo, W., (2007). *SEAWAT Version 4: A computer program for simulation of multi-species solute and heat transport*: U.S. Geological Survey Techniques and Methods. Book 6, Chapter A22, 39 p.
- Li, L., Barry, D. A., Stagnitti, F., & Parlange, J.-Y. (1999). Submarine groundwater discharge and associated chemical input to a coastal sea. *Water Resources Research*, 35(11), 3253–3259.
- Luyun, R., Jr., Momii, K., & Nakagawa, K. (2009). Laboratory-scale saltwater behavior due to subsurface cutoff wall. *Journal of Hydrology*, 377, 227–236.
- Mao, X., Prommer, H., Barry, D. A., Langevin, C. D., Panteleit, B., & Li, L. (2006). Three-dimensional model for multi-component reactive transport with variable density groundwater flow. *Environmental Modeling & Software*, 21(5), 615–628.
- Mastrocicco, M., Colombani, N., & Petitta, M. (2011). Modeling the density contrast effect on a chlorinated hydrocarbon plume reaching the shore line. *Water, Air, and Soil Pollution*, 220(1), 387–398.
- Moore, W. S. (1999). The subterranean estuary: A reaction zone of groundwater and seawater. *Marine Chemistry*, 65, 111–125.
- Naji, A., Ouazar, D., & Cheng, A. H. D. (1998). Locating the saltwater-freshwater interface using nonlinear programming and *h*-adaptive BEM. *Engineering Analysis with Boundary Elements*, 21(3), 253–259.
- Netzer, L., Weisbrod, N., Kurtzman, D., Nasser, A., Graber, E. R., & Ronen, D. (2011). Observations on vertical variability in groundwater quality: Implications for aquifer management. *Water Resources Management*, 25, 1315–1324.
- Oude Essink, G. H. P. (2001). Salt water intrusion in a three-dimensional groundwater system in The Netherlands: A numerical study. *Transport in Porous Media*, 43(1), 137–158.
- Praveena, S. M., & Aris, A. Z. (2010). Groundwater resources assessment using numerical model: A case study in low-lying coastal area. *International journal of Environmental Science and Technology*, 7(1), 135–146.
- Reilly, T. E., & Goodman, A. S. (1985). Quantitative analysis of saltwater–freshwater relationships in groundwater systems—A historical perspective. *Journal of Hydrology*, 80, 125–160.
- Robinson, M. A., Gallagher, D. L., & Reay, W. (1998). Field observations of tidal and seasonal variations in ground water discharge to tidal estuarine surface water. *Ground Water Monitoring and Remediation*, 18, 83–92.
- Sammari, C., Koutitonsky, V. G., & Moussa, M. (2006). Sea level variability and tidal resonance in the Gulf of Gabes, Tunisia. *Continental Shelf Research*, 26, 338–350.
- Shoemaker, W. B. (2004). Important observations and parameters for a salt water intrusion model. *Ground Water*, 42(6–7), 829–840.
- Simmons, G. M. (1992). Importance of submarine groundwater discharge (SGWD) and seawater cycling to material flux across sediment/water interface in marine environments. *Marine Ecology Program Series*, 84, 173–184.
- Simmons, C. T., Fenstemaker, T. R., & Sharp, J. M., Jr. (2001). Variable-density groundwater flow and contaminant transport in heterogeneous porous media: Approaches, resolutions and future challenges. *Journal of Contaminant Hydrology*, 52(1–4), 245–275.
- Ullman, W. J., Chang, B., Miller, D. C., & Madsen, J. A. (2003). Groundwater mixing, nutrient diagenesis, and discharges across a sandy beachface, Cape Henlopen, Delaware (USA). *Estuarine, Coastal and Shelf Science*, 57, 539–552.
- Valiela, I., Foreman, K., LaMontagne, M., Hersh, D., Costa, J., Peckol, P., et al. (1992). Coupling of watersheds and coastal waters: Sources and consequences of nutrient enrichment in Waquoit Bay, Massachusetts. *Estuaries*, 15(4), 443–457.
- Volker, R. E., Zhang, Q., & Lockington, D. A. (2002). Numerical modeling of contaminant transport in coastal aquifers. *Mathematics and Computers in Simulation*, 59, 35–44.
- Weiskel, P. K., & Howes, B. L. (1992). Differential transport of sewage derived nitrogen and phosphorous through a coastal watershed. *Environmental Science and Technology*, 26, 352–360.
- Xue, Y., Xie, C., Wu, J., Lie, P., Wang, J., & Jiang, Q. (1995). A 3-dimensional miscible transport model for seawater intrusion in China. *Water Resources Researches*, 31(4), 903–912.
- Zhang, Q., Volker, R. E., & Lockington, D. A. (2001). Influence of seaward boundary condition on contaminant transport in unconfined coastal aquifers. *Journal of Contaminant Hydrology*, 49, 201–215.
- Zhang, Q., Volker, R. E., & Lockington, D. A. (2002). Experimental investigation of contaminant transport in coastal groundwater. *Advances in Environmental Research*, 6, 229–237.
- Zheng, C., & Bennett, G. D. (2002). *Applied contaminant transport modeling* (2nd ed., p. 621). New York: John Wiley & Sons.